

# Transcriptional regulation of miR-483-3p mediated by IL-6/STAT3 axis promoted epithelial-mesenchymal transition and tumor stemness in glioma

Donghui Xu<sup>1,\*</sup>, Guonan Chi<sup>1,\*</sup>, Dejun Xu<sup>2</sup>

<sup>1</sup>Department of Neurosurgery, China-Japan Union Hospital of Jilin University, Changchun, Jilin Province, China

<sup>2</sup>Department of Lymphovascular Surgery, China-Japan Union Hospital of Jilin University, Changchun, Jilin Province, China

\*Equal contribution

Correspondence to: Dejun Xu; email: [Xudj@jlu.edu.cn](mailto:Xudj@jlu.edu.cn)

Keywords: glioma, miR-483-3p, EMT, stemness, IL6

Received: April 16, 2020

Accepted: July 6, 2020

Published: November 4, 2020

**Copyright:** © 2020 Xu et al. This is an open access article distributed under the terms of the [Creative Commons Attribution License](https://creativecommons.org/licenses/by/3.0/) (CC BY 3.0), which permits unrestricted use, distribution, and reproduction in any medium, provided the original author and source are credited.

## ABSTRACT

**Background:** MiRNA can be involved in regulating tumor genesis and development through regulating the major genes expression and regulating corresponding pathways. Here, we investigated the function and mechanisms of miR-483-3p in glioma progression.

**Results:** We found that miR-483-3p was increased in glioma cells and tissues. Silencing of miR-483-3p attenuated glioma progression and stemness. STAT3 activation which was induced by IL6 mediated the transcription of miR-483-3p gene.

**Conclusion:** The present study indicated miR-483-3p acting as a tumorigenesis gene regulated by IL6/STAT3 axis, thus providing more experimental basis for clinical treatment of glioma.

**Methods:** qRT-PCR was performed to measure miR-483-3p level. Transwell assay, wound healing assay, flow cytometry and immunofluorescence are used to detect the role of miR-483-3p in migration, invasion, epithelial-mesenchymal transition (EMT) and stemness in glioma cells. Western blot analysis was performed to analyze protein level. Luciferase assay was performed to examine the interaction between miR-483-3p and STAT3.

## INTRODUCTION

A glioma is a malignant brain tumor caused by the malignant transformation of glioma cells in the spinal cord and brain [1–4]. According to the origin of tumor, glioma can be divided into astrocytoma, which is the major type of glioma, glioblastoma, medulloblastoma, ependymoma and oligodendroglioma [5]. Glioma is characterized by the invasive growth, abundant blood vessels and high recurrence rate. Those characters make it difficult to diagnosis the development of glioma patients and also contributes to the low effectiveness of long-term neurosurgery [6]. The higher the pathological grade of glioma, the stronger its invasion, the more blurred the boundary between tumor tissue and normal

brain tissue, greatly increasing the difficulty of surgical resection and chemoradiotherapy resistance [4, 6–8]. The development of treatment methods and therapeutic drugs and the improvement of diagnostic standards does not make the condition of glioma patients better in recent years. The five-year survival rates for patients with glioma are still lower than 3 percent [9]. Glioma is a kind of polygenic lesion disease. Multiple genes contribute to the occurrence and development of glioma. It is very meaningful to investigate the level changes of genes in glioma.

MicroRNA (miRNA) is a group of small RNA with a length of about 18-24 NT encoded by animal, plant and virus genomes. MiRNA is highly conserved in evolution.

It can inhibit the translation or degradation of target gene by combining with 3'-UTR of target gene [10–12]. In recent years, studies have confirmed that miRNA, through its post transcriptional mechanism, participates in embryonic development, cell differentiation, proliferation and apoptosis and is important for the development of tumor [13, 14]. Functions of miRNAs are widely reported in glioma. miR-93 acts as a cancerogenic miRNA and promotes invasion and migration of glioma cells via targeting RBL2 [1]. Contrarily, miR-320a directly targets aquaporin 4 to inhibit glioma process [15]. Jiang et al. found that migration and proliferation of glioma cells can be inhibited by miR-214 by targeting caspase 1 [16]. Those previous findings suggest us the important roles of miRNAs in glioma.

MiR-483-3p was first described to be increased in malignant mesothelioma [17]. Then, Bertero T et al. indicated that overexpression of miR-483-3p promotes wounded epithelial cells proliferation [18]. Furthermore, miR-483-3p induces apoptosis of endothelial cells and macrophages and impairs the ability of endothelial regeneration [19]. Besides, miR-483-3p contributes to alleviation of breast cancer proliferation and progression [20]. However, the mechanism of miR-483-3p in glioma is still poorly understood.

Here we want to explore the functions of miR-483-3p in glioma process, which might contribute to a potential drug target for glioma treatment.

## RESULTS

### MiR-483-3p levels in different glioma cell lines and in glioma tissue of human and mice

To examine the role of miR-483-3p in glioma, we firstly detected its expression level in glioma tissues and cells. As shown in Figure 1A, we collected cancer and para-cancer normal tissues from 50 glioma patients. MiR-483-3p was up-regulated in cancer tissues than that in adjacent normal tissues (Figure 1A). Then, we examined miR-483-3p level in mice with glioma. The difference of miR-483-3p between cancer tissues and adjacent normal tissues is similar to that in human tissues (Figure 1B). Meanwhile, we also detected miR-483-3p levels in different glioma cell lines. As shown in Figure 1C, miR-483-3p was increased in U251 and U87 cells. However, only slight increase of miR-483-3p were found in A172 and SHG44 cells compared to the normal human astrocytes (NHA) (Figure 1C). Kaplan-Meier curves were used to compare the total survival of patients with low and high miR-483-3p level. The 5-year survival rate of high miR-483-3p level patients was lower than low level patients (Figure 1D).

### miR-483-3p silencing suppressed glioma cell EMT process

As shown in Figure 1C, U251 and U87 cells own the highest miR-483-3p level, and we chose U251 and U87 to perform the following experiments. To further explore the function of miR-483-3p in glioma process, we constructed AMO-483-3p and transfected it into U251 and U87 cells to inhibit miR-483-3p level. In addition, AMO-483-3p significantly reduced the level of miR-483-3p in U251 and U87 cells (Figure 2A and 2D). We firstly investigated the effect of miR-483-3p on epithelial-mesenchymal transition (EMT) of glioma. Glioma is different from other epithelial-type tumors. The absence of epithelial cell structure lead to the poorly expression of E-cadherin. Therefore, we detected the level changes of Vimentin, E-cadherin and N-cadherin, the mesenchymal phenotype markers, and TWIST, the key transcription factor responsible for EMT, to evaluate the EMT process in glioma. We found that miR-483-3p silencing by transfection of AMO-483-3p significantly reduced the protein levels of Vimentin, TWIST and N-cadherin and elevated the level of E-cadherin in U251 and U87 cells (Figure 2B and 2E). In addition, immunofluorescence was also performed to detect the Vimentin level. As shown in Figure 2C and 2F, Vimentin positive staining cells were decreased due to miR-483-3p silencing.

### miR-483-3p silencing attenuated invasion and migration of glioma cells

Next, we determined the effect of miR-483-3p in invasion and migration process in U251 and U87 cells. Transwell assay was performed to determine the invasion of U251 and U87 cells. AMO-483-3p transfection significantly attenuated the invasion of glioma cells (Figure 3A and 3C). However, the negative control group didn't show such effect. Then, wound healing assay was performed to examine the role of miR-483-3p in migration process. We found that miR-483-3p silencing suppressed the migration of U251 and U87 cells (Figure 3B and 3D).

### miR-483-3p promoted glioma cells stemness.

Cancer cell stemness contributes to the development of malignant tumor. We constructed the overexpression plasmid of miR-483-3p to elevated miR-483-3p level in U251 cells (Figure 4A). Then, qRT-PCR analysis was performed to measure the mRNA level of the markers of stem cell. As shown in Figure 4B–4H, the mRNA levels of CD44, CD133, ALDH-1, Oct4, Nanog, Sox2 and Snail was upregulated by the overexpression of miR-483-3p and significantly inhibited after the transfection of AMO-483-3p. Conversely, the mRNA

level of CD24 was reduced after overexpression of miR-483-3p and increased by the AMO-miR-483-3p transfection (Figure 4I). Flow cytometry was used to analyze the mammospheres, the CD44(+)/CD24(-) subpopulations were more abundant in miR-483-3p overexpression group than the controls (19.7%) (Figure 4J). Contrarily, the CD44(-)/CD24(+) subpopulations were higher in AMO-NC group (94.3%) than that in miR-483-3p inhibition group (78.9%) (Figure 4J). Furthermore, we examined protein levels of part of those markers. Nanog and Snail were upregulated by miR-483-3p upregulation and they were decreased after miR-483-3p silencing (Figure 4K).

### STAT3 was activated in U251 and U87 cells.

The mechanisms of miRNAs played were widely reported in cancer. Here we wanted to investigate the upstream of miR-483-3p expression. As shown in Figure 5A, we collected cancerous and para-cancer normal tissue from 39 glioma patients, qRT-PCR analysis was performed to test mRNA level of STAT3. We found that STAT3 was up-regulated in cancer

tissues. We also measure the mRNA level of STAT3 in different glioma cell lines. We found that the mRNA of STAT3 was significantly elevated in U251 and U87 cells (Figure 5B). The protein levels of phosphorylated and total STAT3 was also detected and the ratio of p-STAT3/STAT3 was significantly increased in U251 and U87 cells (Figure 5C).

### STAT3 transcriptional upregulated miR-483-3p level in U251 cells

Then we examined whether STAT3 mediated miR-483-3p expression. Gain- and loss-of-function experiments were performed. We found that knockdown of STAT3 using siRNA of STAT3 reduced miR-483-3p level and forced expression of STAT3 by expression plasmid increased miR-483-3p level (Figure 6A and 6B). To further investigate if STAT3 mediated miR-483-3p expression via transcription factor function, luciferase assay was performed to examine the relationship between miR-483-3p and STAT3. As shown in Figure 6C, STAT3, which had no effect on the vector that carries mutated the binding site (Mut-miR-483-3p),

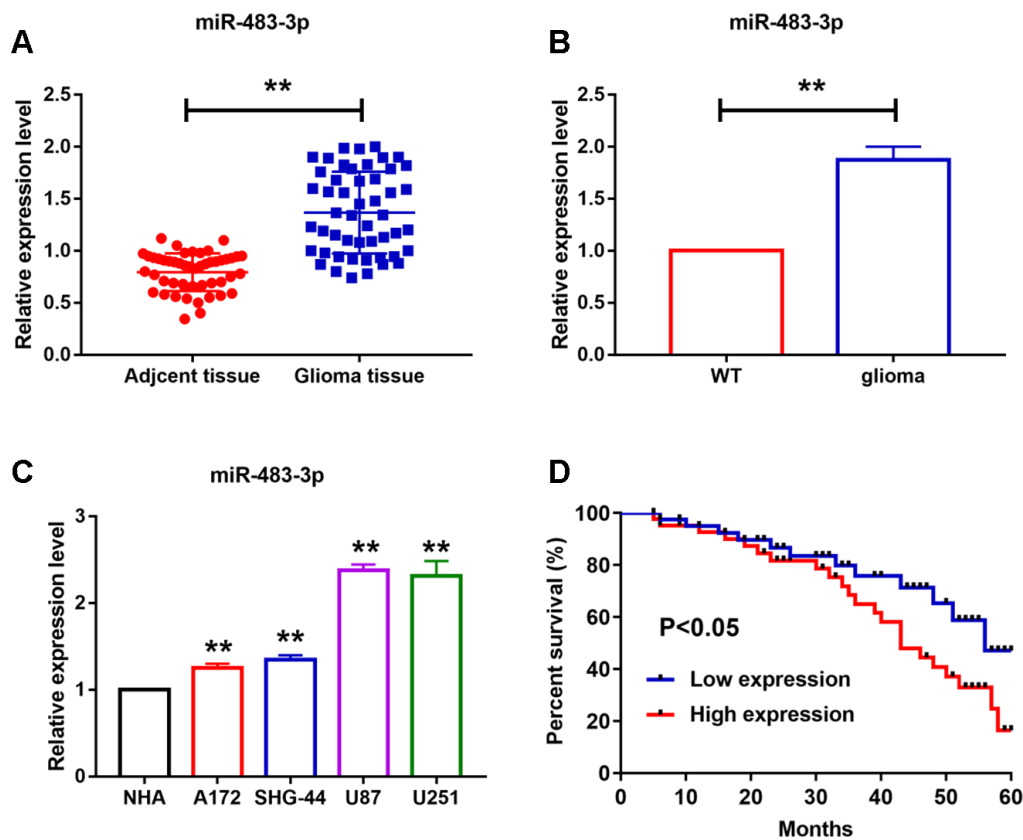


**Figure 1. MiR-483-3p levels in different glioma cell lines and in glioma tissue of human and mice.** (A–C) qRT-PCR analysis showed upregulation of miR-483-3p in cancer tissues and different cancer cell lines. Data are mean ± SEM; Two-tailed t test was used for the statistical analysis. n= 50 glioma patients or 6 mice per group or 5 independent cell cultures. (D) The 5-year survival rate of high and low miR-483-3p level patients. Data are mean ± SEM; Two-tailed t test was used for the statistical analysis. \*\*P<0.05.

elevated the activity of wild-type miR-483-3p luciferase vector (WT-miR-483-3p).

### IL6/STAT3 axis activation increased miR-483-3p expression

We then explore the effect of STAT3 phosphorylation to miR-483-3p expression. As shown in Figure 7A and 7D, treatment of STAT3 phosphorylation inhibitor, SH-4-54, significantly inhibited the expression of miR-483-3p. Besides, the inhibitory efficiency of SH-4-54 was also evaluated. Treatment of SH-4-54 significantly reduced the level of STAT3 phosphorylation in U251 and U87

cells (Figure 7B and 7E). IL6 was reported to activate the phosphorylation of STAT3. Here we investigated whether IL6 mediated miR-483-3p expression. Expression plasmid of IL6 was constructed to forced express IL6 in U251 and U87 cells (Figure 7C and 7F). Then, miR-483-3p was determined. As shown in Figure 7C and 7F, neutralization of IL-6 by neutralizing antibody (NA) inhibited the expression of miR-483-3p and IL-6 overexpression elevated miR-483-3p level, which was reversely inhibited by SH-4-54, and DMSO group showed no such effect. Taken together, these data indicated that the expression of miR-483-3p was transcriptional regulated by the IL6/STAT3 axis.

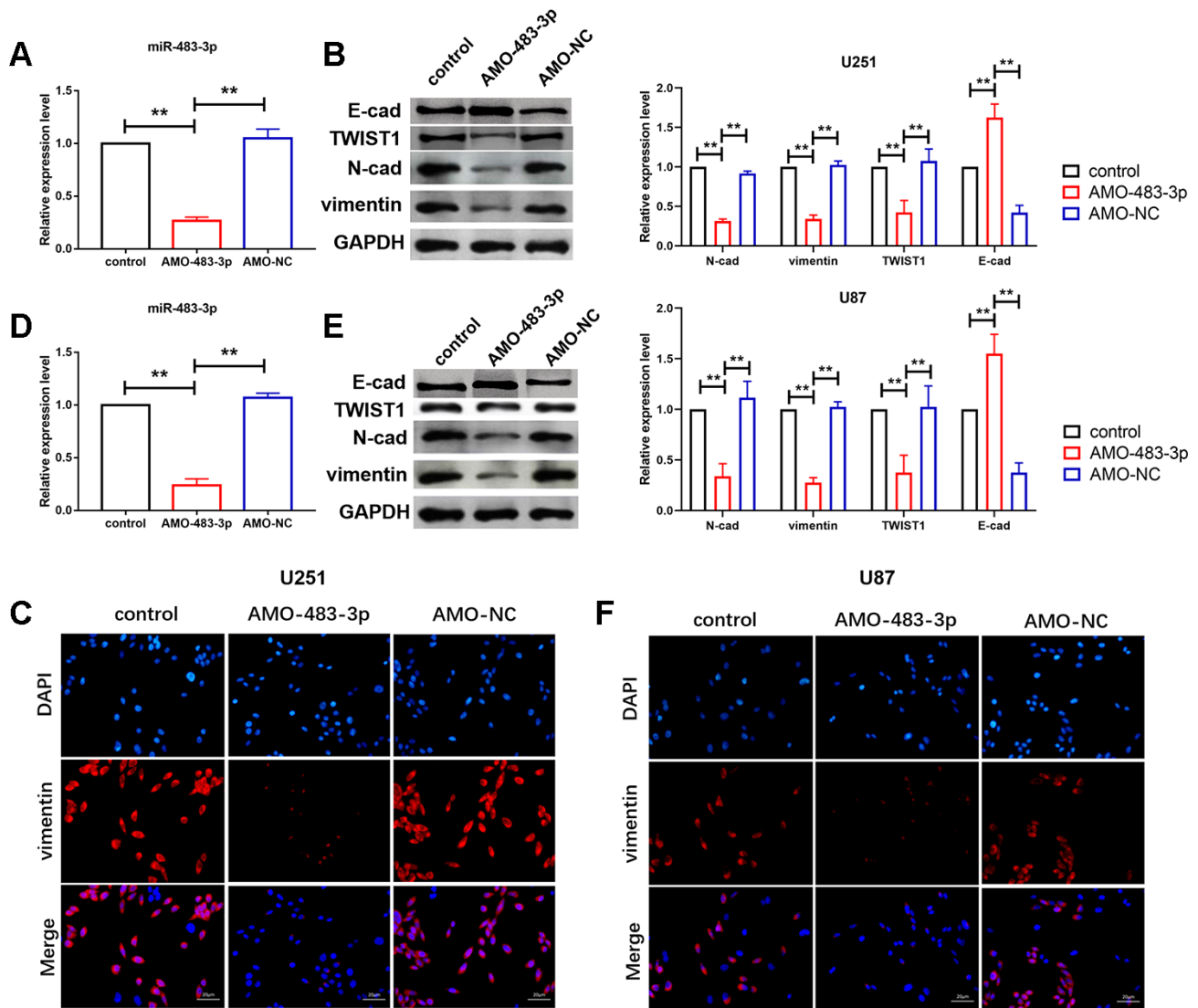


**Figure 2. miR-483-3p silencing suppressed glioma cell EMT process.** (A, D) qRT-PCR analysis showed efficiency of AMO-483-3p in U251 and U87 cells. Data are mean  $\pm$  SEM; one-way ANOVA was used for the statistical analysis. n=5 independent cell cultures. (B, E) Western blot analysis showed reduction of protein levels of vimentin and TWIST, E-cad and N-cad of in U251 and U87 cells. Data are mean  $\pm$  SEM; one-way ANOVA was used for the statistical analysis. n=5 independent cell cultures. (C, F) Immunostaining of vimentin in U251 and U87 cells. n=4 independent cell cultures. \*\*P<0.05.

### MiR-483-3p promoted in vivo tumor growth in the nude mice

To investigate the role of miR-483-3p on tumorigenesis of glioma, we set up xenograft nude mice model. Stable miR-483-3p transfected U251 cell lines were

constructed and were injected into nude mice via tail veins. Then tumor volume was measured. The mice injected normal U251 cells showed a smaller tumor volume and tumors grew faster when forcing expression of miR-483-3p (Figure 8A). The tumors were isolated at 30 days after injection, miR-483-3p significantly

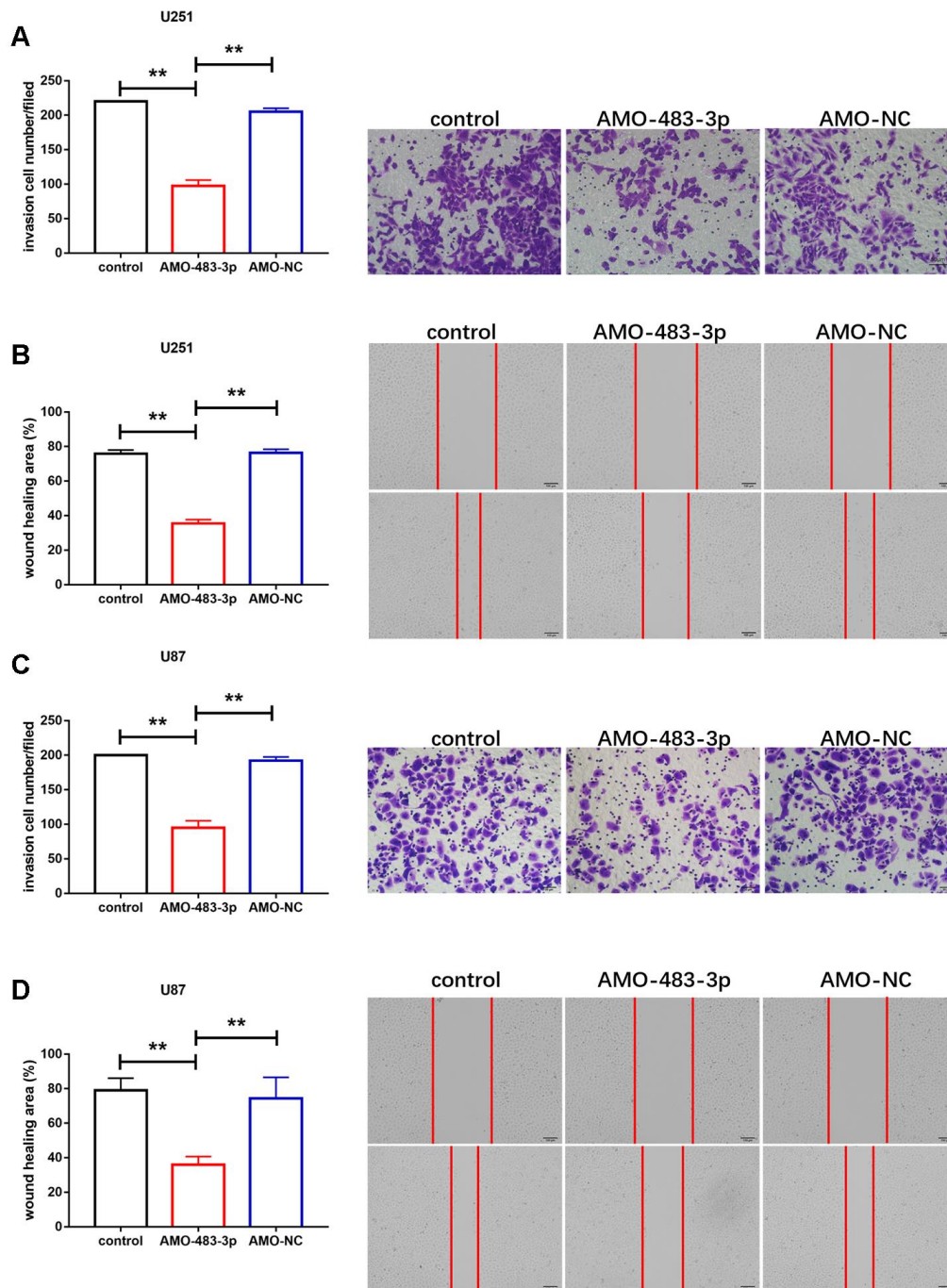


**Figure 3. miR-483-3p silencing attenuated invasion and migration of glioma cells.** (A, C) Effect of AMO-483-3p on invasion of U251 and U87 cells. Data are mean  $\pm$  SEM; one-way ANOVA was used for the statistical analysis. n=5 independent cell cultures. (B, D) Wound healing assay of U251 and U87 cells. Data are mean  $\pm$  SEM; one-way ANOVA was used for the statistical analysis. n=5 independent cell cultures. \*\*P<0.05.

increased tumors weight (Figure 8B). In addition, these tumor tissues were isolated to identified miR-483-3p level. And we found that expression level of miR-483-3p was increased in stable miR-483-3p transfected U251 cell lines injection mice (Figure 8C).

Next, we examined the effect of miR-483-3p on glioma migration. And we found that miR-483-3p increased the mRNA and protein levels of EMT related markers N-cadherin, vimentin and TWIST1 and decreased the mRNA and protein levels of E-cadherin in tumor tissues (Figure 8D and 8E). Furthermore, miR-483-3p significantly promoted pulmonary metastasis of glioma compared with NC group (Figure 8F). These results suggested us the important role of miR-483-3p on tumor growth and migration.

## DISCUSSION

Glioma is one of the common central neural system tumors. The etiology that causes this disease is not clear, with tumor origin, genetic factor, biochemical environment, ionizing radiation, nitroso compound, polluted air, bad life habit, infection and other factors concerned. Even with current treatments that include maximum tumor removal and combined chemoradiotherapy, the prognosis for glioma patients is very poor and only 3% to 5% of patients likely to survive longer [21]. Therefore, it is urgent to explore the pathogenesis of glioma and provide targeted therapy strategies from the molecular perspective.

MicroRNA (miRNA) is a kind of endogenous RNA found in eukaryotic cells in recent years. It participates

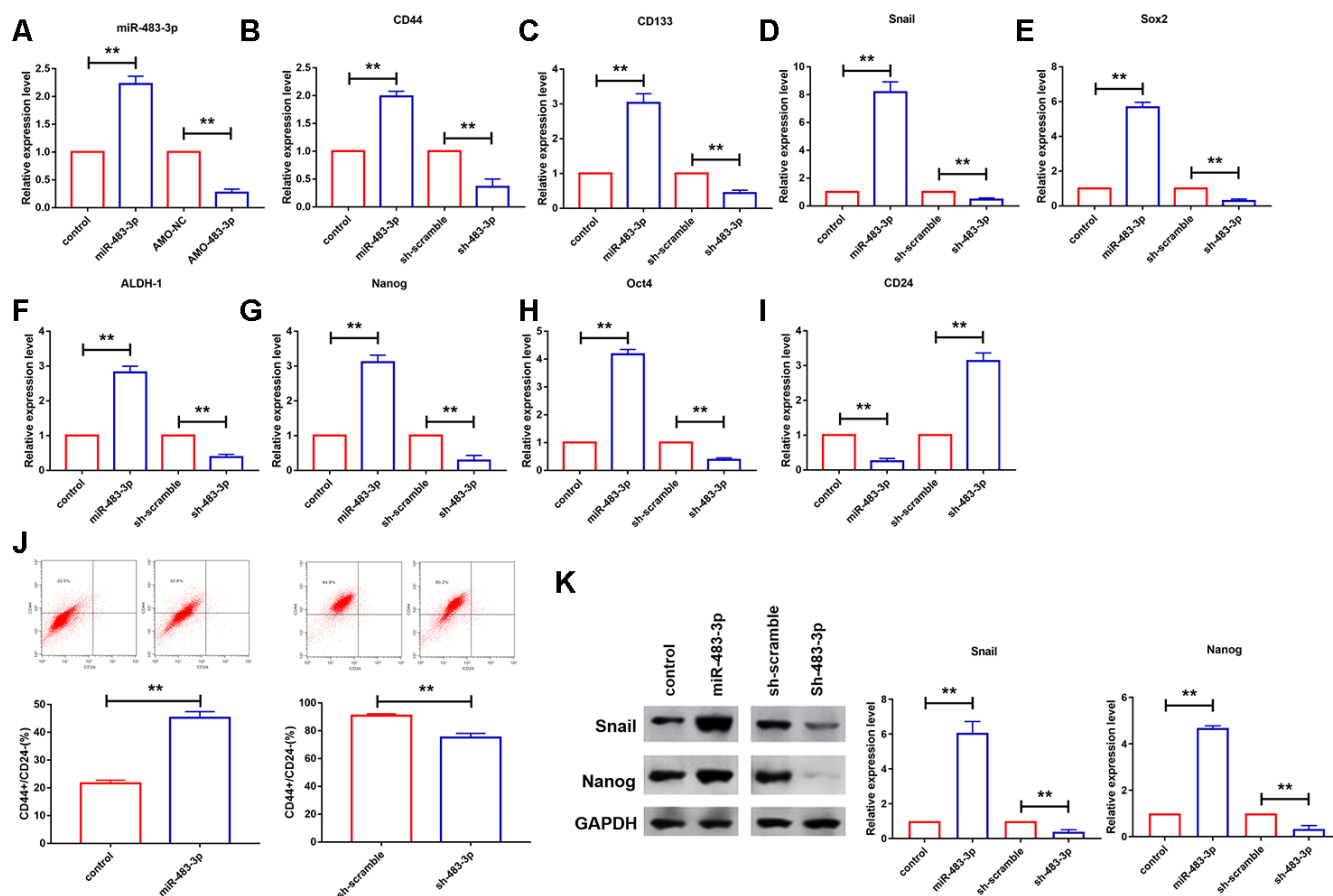


**Figure 4. miR-483-3p promoted glioma cells stemness.** (A) qRT-PCR analysis showed efficiency of AMO-483-3p and miR-483-3p in U251 cells. Data are mean  $\pm$  SEM; Two-tailed t test was used for the statistical analysis. n=5 independent cell cultures. (B–I) qRT-PCR analysis showed the mRNA levels of CD44, CD133, Snail, Sox2, ALDH-1, Nanog, Oct4 and CD24 in U251 cells. Data are mean  $\pm$  SEM; Two-tailed t test was used for the statistical analysis. n=5 independent cell cultures. (J) representative flow cytograms of the expression of CD24 and CD44. Data are mean  $\pm$  SEM; Two-tailed t test was used for the statistical analysis. n=5 independent cell cultures. (K) Western blot analysis showed reduction of protein levels of Nanog and Snail in U251 cells. Data are mean  $\pm$  SEM; Two-tailed t test was used for the statistical analysis. n=5 independent cell cultures. \*\*P<0.05.

in cell proliferation, differentiation, apoptosis and disease development etc. Fang et al. found that miRNA-188-5p inhibits hepatocellular carcinoma cells proliferation and migration via targeting FGF5 [21]. MiRNA-7 was identified to mediate TRAIL induced glioblastoma cells apoptosis and inhibit tumor growth [22]. Previous studies showed that tumor process can be regulated by miR-483-3p. Wu et al. found miR-483-3p targets PUMA to promote cell migration and proliferation in neuroblastoma [23]. Furthermore, miR-483-3p elevation facilitates colony formation, proliferation and growth of pancreatic ductal adenocarcinoma (PDAC) cells [24]. However, miR-483-3p can also act as a suppressor of breast cancer by reducing the expression of HDAC8. Here we found that miR-483-3p level was elevated in glioma tissues of clinical patients and mice and in glioma cell lines. Furthermore, silencing of miR-483-3p inhibited glioma cells migration and invasion of in vitro. The stemness features of cancer stem cells are attributed to numerous

signaling pathway, such as differentiation, self-renewal, epithelial to mesenchymal transition (EMT) and migration etc. CSCs can originate from cancer cells which have endured epithelial-mesenchymal transition (EMT) process [25]. Here we indicated that alleviation of miR-483-3p suppresses the EMT process of glioma cells. Moreover, we also detected increased protein levels of stem cell markers in miR-483-3p over-expressed glioma cells, which demonstrated that miR-483-3p promotes the glioma stemness. However, silencing of miR-483-3p only caused the mild decrease in CD44(-)/CD24(+) subpopulations. It gives us a suggestion that glioma cell may has the compensatory action that contributes to stemness and attenuates the influence of inhibition of single miRNA. In addition, we also predicted the target genes of miR-483-3p using target scan ([http://www.targetscan.org/vert\\_72/](http://www.targetscan.org/vert_72/)) and will further detected the function of downstream genes of miR-483-3p in our next study (Supplementary Table 1).

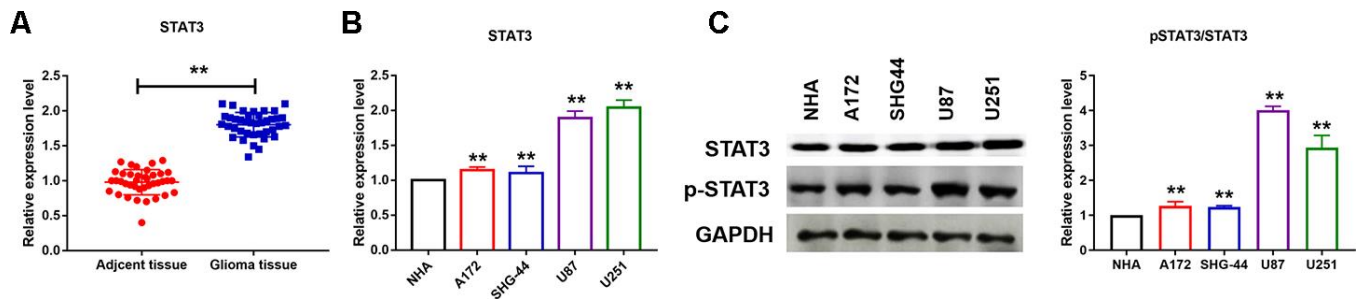


**Figure 5. STAT3 was activated in U251 and U87 cells.** (A, B) qRT-PCR analysis showed upregulation of STAT3 in cancer tissues and different cancer cell lines. Data are mean  $\pm$  SEM; Two-tailed t test was used for the statistical analysis. n= 39 glioma patients or 5 independent cell cultures. (C) Western bolt analysis showed protein levels of STAT3 in different cancer cell lines. Data are mean  $\pm$  SEM; Two-tailed t test was used for the statistical analysis. n=5 independent cell cultures. \*\*P<0.05.

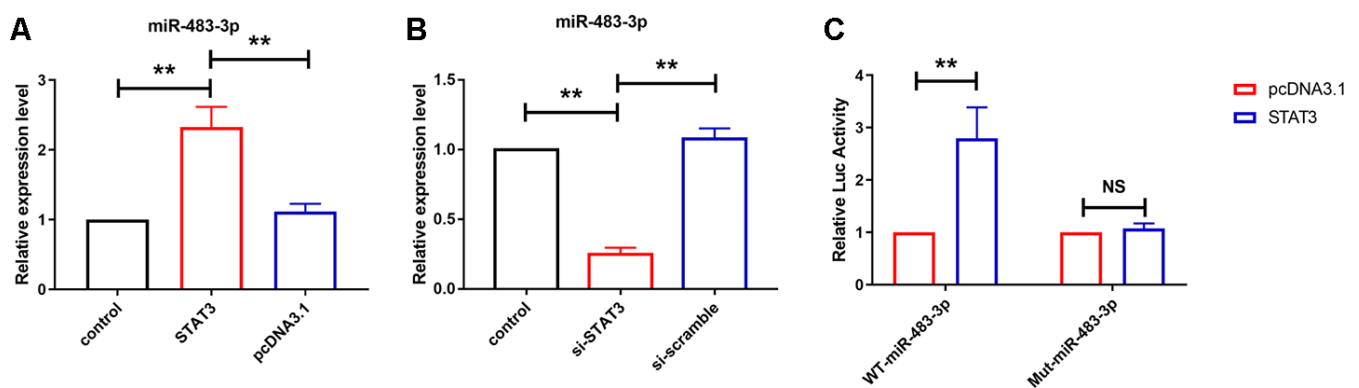


**Figure 6. STAT3 transcriptional upregulated miR-483-3p level in U251 cells.** (A, B) qRT-PCR analysis showed the expression level of miR-483-3p in U251 cells after overexpression and knockdown of STAT3. Data are mean  $\pm$  SEM; one-way ANOVA was used for the statistical analysis. n=5 independent cell cultures. (C) Luciferase reporter activities of chimeric vectors carrying the luciferase gene and a fragment of the 3' UTR of miR-483-3p containing the wild type or mutant STAT3 binding sites. Data are mean  $\pm$  SEM; Two-tailed t test was used for the statistical analysis. n=5 independent cell cultures. \*\*P<0.05

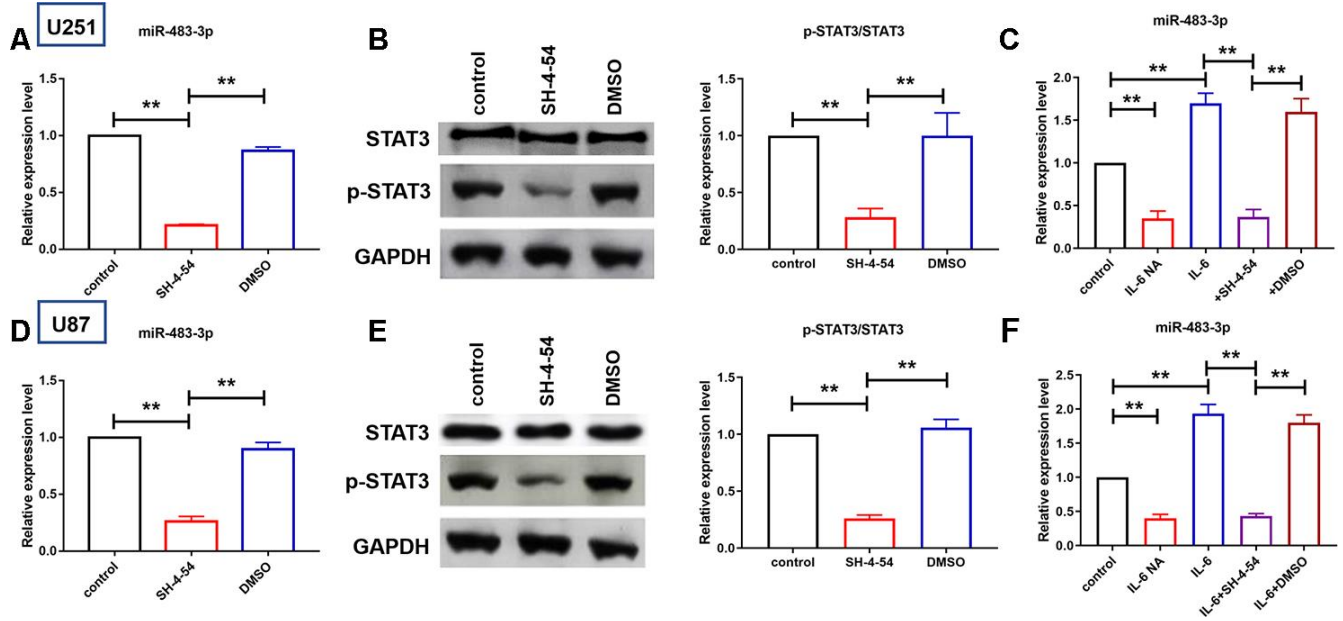


**Figure 7. IL6/STAT3 axis activation increased miR-483-3p expression.** (A, D) qRT-PCR analysis showed the expression level of miR-483-3p in U251 and U87 cells after treatment of STAT3 phosphorylation inhibitor. Data are mean  $\pm$  SEM; one-way ANOVA was used for the statistical analysis. n=5 independent cell cultures. (B, E) Western blot analysis showed protein levels of p-STAT3 and total STAT3 in U251 and U87 cells. Data are mean  $\pm$  SEM; one-way ANOVA was used for the statistical analysis. n=5 independent cell cultures. (C, F) qRT-PCR analysis showed the expression level of miR-483-3p in U251 and U87 cells after IL-6 overexpression and neutralization and STAT3 inhibition. Data are mean  $\pm$  SEM; one-way ANOVA was used for the statistical analysis. n=5 independent cell cultures. \*\*P<0.05.

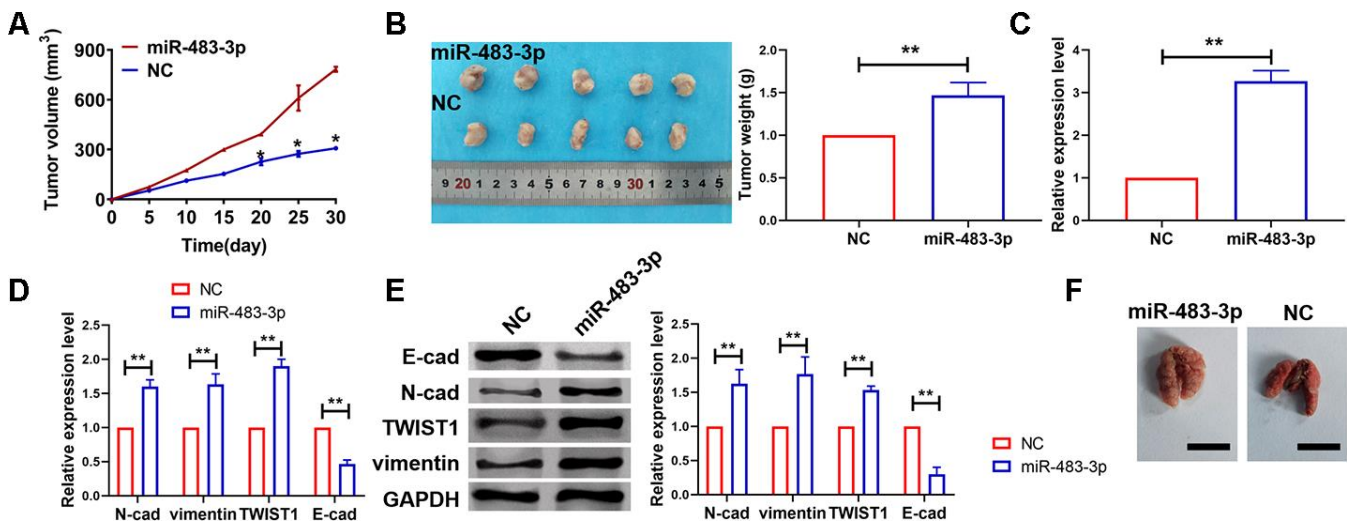


**Figure 8. miR-483-3p promoted in vivo tumor growth in the nude mice.** (A) Tumor volume was increased after miR-483-3p overexpression. Data are mean  $\pm$  SEM; Two-tailed t test was used for the statistical analysis. n=5 mice. (B) Tumor weight was increased after miR-483-3p overexpression. Data are mean  $\pm$  SEM; Two-tailed t test was used for the statistical analysis. n=5 mice. (C) RT-PCR showed miR-483-3p level. Data are mean  $\pm$  SEM; Two-tailed t test was used for the statistical analysis. n=6 mice. (D) RT-PCR showed mRNA level of EMT related markers. Data are mean  $\pm$  SEM; Two-tailed t test was used for the statistical analysis. n=5 mice. (E) Western blot showed protein level of EMT markers. Data are mean  $\pm$  SEM; Two-tailed t test was used for the statistical analysis. n=5 mice. (F) Pulmonary metastasis of glioma was detected. n=5 mice.

Abnormal activation of STAT3 promotes tumorigenesis. Expression of protein coding genes induced by STAT3 has been widely explored. However, transcription of miRNA gene regulated by STAT3 in glioma tumorigenesis is poorly understood. Jianfei Xue et al. indicated that activation of STAT3 transcriptional regulates the expression of miR-182-5p and promotes tumorigenesis of glioma [26]. Our study demonstrated that elevation of miR-483-3p is induced by transcriptional regulation of STAT3. Chronic inflammation is a kind of important factor for tumor development and progression. IL6 is widely known as a critical mediator of inflammation and high level of IL6 can be observed in tumor microenvironment [27]. We found that IL6 activates STAT3 in glioma cells and promotes miR-483-3p upregulation.

At present, studies on the molecular level of glioma are still insufficient. Whether it can provide a new way for the development of cancer treatment drugs, these will be a long way to go. It is believed that with the further investigation of miRNA in glioma, these problems will be gradually solved, which will bring new opportunities for clinical diagnosis and treatment.

## CONCLUSION

Our study indicated that miR-483-3p acted as a novel factor in regulation of glioma cell invasion, migration, EMT and stemness. IL6/STAT3 axis mediates the transcription of miR-483-3p. Furthermore, forced expression of miR-483-3p promoted tumor growth and migration. On this basis, more prospective studies should be carried out to promote the early detection and treatment and prediction of the prognosis of glioma.

## MATERIALS AND METHODS

### Clinical samples

Fresh adjacent normal tissue samples and glioma tissue samples were taken from glioma patients undergoing surgical procedures at China-Japan Union Hospital of Jilin University. All of the patients or their guardians provided written consent, and the Ethics Committee of China-Japan Union Hospital of Jilin University.

### In vivo tumor growth assay

Nude mice were purchased from Guangdong provincial experimental animal center for medicine. U251 cells ( $5 \times 10^6$ ) were subcutaneously injected in right lower limb of the nude mice or through abdominal and vail veins. Tumor size was measured every five days. After 30 days of injection, the tumor

or lungs was removed for follow-up study. 7 days before injection, AAV-miR-483-3p or its NC was injected into mice via tail veins.

### Cell culture

The cell lines were purchased from the Science Cell Laboratory. Cells were cultured in PRIM 1640 (GIBCO, USA) supplemented with 10 % fetal bovine serum (Cromwell, USA) and 100  $\mu$ L/mL penicillin and streptomycin (Sigma-Aldrich, USA) and placed at 37°C with 5% CO<sub>2</sub>.

### Transfection

For STAT3 and IL6 overexpression, full-length STAT3 and IL6 were amplified and sub-cloned into pcDNA3.1, and stable clones were obtained with G418. pcDNA3.1 empty vector was used as a negative control. For STAT3 knockdown, siRNA targeting STAT3 and a scrambled siRNA used as negative control (nc) were synthesized. All plasmids were isolated using AxyPrep DNA Miniprep Kit (Axygen, USA). The miR-483-3p inhibitors and respective negative controls were produced by RiboBio (Guangzhou, China). HEK293 and glioma cell lines were transfected according to the protocol from manufacturer. Six hours later, we changed the transfection medium to culture medium with 10% FBS. 2  $\mu$ M of SH-4-54 (selleckchem) was treated into cells for 24h in 6-wells plates [28].

### RNA isolation and qRT-PCR

Total RNA was isolated from tissue and cells according to a standard protocol. And then, the purity and concentration of RNA was detected and all the samples were converted into cDNA using reverse transcription kit. We used SYBR Green (Thermo Fisher Scientific) system to perform the qRT-PCR. Data was analyzed by GraphPad 7.

### Western blot

Protein samples were blotted depended on standard protocol. And we used Odyssey Infrared Scanning System (Gene Co. Ltd., Hongkong, China) to scan the membranes. At last, we used Image J software to analyze the western bolt results.

The antibodies are as list:

Vimentin antibody was produced by Abcam (MA, USA). Snail and N-cadherin antibody were produced by Proteintech Group (Wuhan, China). The secondary antibodies IRDye700/800 Mouse or Rabbit were produced by LICOR (Lincoln, Nebraska, USA).

## Luciferase reporter assay

To identify interaction of STAT3 and miR-483-3p, psiCHECK-2 luciferase reporter plasmid was inserted with the wildtype miR-483-3p-3'UTR or mutant miR-483-3p-3'UTR sequences that contain the putative binding sites of STAT3. scramble or STAT3 expression plasmid were transfected with reporter vectors into glioma cell lines. The cells were collected after 48 h post-transfection and lysed to detect the luciferase activity using Dual-Luciferase Assay System.

## Wound healing assay

$5 \times 10^5$  cells were planted in a 6-well plate, and when the cells grew to fuse, two vertical parallel lines were drawn with 10  $\mu$ L suction head against the ruler. We used PBS to wash the floating cells, and then, cells were cultured in culture medium (serum-free) for 24 hours. Images were taken at 0 and 24 hours of cell culture, respectively.

## Transwell assay

Cells in logarithmic growth phase were adjusted to  $2 \times 10^5$  cells/well of medium (without serum) and plated into the upper chamber insert pre-coated with 1  $\mu$ g/ $\mu$ L Matrigel. Lower chamber was added with 500  $\mu$ L of medium (with 10% FBS), and then incubate the chamber at 37°C for 48 h. Then the invading cells were visualized by the crystal violet and inverted microscope.

## Statistical analysis

The number of independent experimental replications and precisions measures are reported in the figure legends. All data is presented as a mean  $\pm$  S.E.M. Statistical analyses were performed using the GraphPad Prism 7 software and assessed by the two-tailed Student's t test or a one-way ANOVA. P-value < 0.01 was considered as statistically significant.

## CONFLICTS OF INTEREST

The authors declare that there are no conflicts of interest.

## FUNDING

The authors received no funding for this work.

## REFERENCES

1. Liu DK, Wei YJ, Guo Y, Wang J, Wang GH. MiRNA-93 functions as an oncogene in glioma by directly targeting RBL2. *Eur Rev Med Pharmacol Sci.* 2018; 22:2343–50.  
<https://doi.org/10.26355/eurev.201804.14825>  
PMID:29762838
2. Wang W, Zhang A, Hao Y, Wang G, Jia Z. The emerging role of miR-19 in glioma. *J Cell Mol Med.* 2018; 22:4611–16.  
<https://doi.org/10.1111/jcmm.13788>  
PMID:30073755
3. Chen R, Smith-Cohn M, Cohen AL, Colman H. Glioma subclassifications and their clinical significance. *Neurotherapeutics.* 2017; 14:284–97.  
<https://doi.org/10.1007/s13311-017-0519-x>  
PMID:28281173
4. Gusyatiner O, Hegi ME. Glioma epigenetics: from subclassification to novel treatment options. *Semin Cancer Biol.* 2018; 51:50–58.  
<https://doi.org/10.1016/j.semcancer.2017.11.010>  
PMID:29170066
5. Buckner JC, Brown PD, O'Neill BP, Meyer FB, Wetmore CJ, Uhm JH. Central nervous system tumors. *Mayo Clin Proc.* 2007; 82:1271–86.  
<https://doi.org/10.4065/82.10.1271>  
PMID:17908533
6. Bush NA, Chang SM, Berger MS. Current and future strategies for treatment of glioma. *Neurosurg Rev.* 2017; 40:1–14.  
<https://doi.org/10.1007/s10143-016-0709-8>  
PMID:27085859
7. Braunstein S, Raleigh D, Bindra R, Mueller S, Haas-Kogan D. Pediatric high-grade glioma: current molecular landscape and therapeutic approaches. *J Neurooncol.* 2017; 134:541–49.  
<https://doi.org/10.1007/s11060-017-2393-0>  
PMID:28357536
8. Chen J, McKay RM, Parada LF. Malignant glioma: lessons from genomics, mouse models, and stem cells. *Cell.* 2012; 149:36–47.  
<https://doi.org/10.1016/j.cell.2012.03.009>  
PMID:22464322
9. Yekula A, Minciacchi VR, Morello M, Shao H, Park Y, Zhang X, Muralidharan K, Freeman MR, Weissleder R, Lee H, Carter B, Breakefield XO, Di Vizio D, Balaj L. Large and small extracellular vesicles released by glioma cells in vitro and in vivo. *J Extracell Vesicles.* 2019; 9:1689784.  
<https://doi.org/10.1080/20013078.2019.1689784>  
PMID:31839905
10. Mohr AM, Mott JL. Overview of microRNA biology. *Semin Liver Dis.* 2015; 35:3–11.  
<https://doi.org/10.1055/s-0034-1397344>  
PMID:25632930

11. Bushati N, Cohen SM. microRNA functions. *Annu Rev Cell Dev Biol.* 2007; 23:175–205.  
<https://doi.org/10.1146/annurev.cellbio.23.090506.123406> PMID:[17506695](https://pubmed.ncbi.nlm.nih.gov/17506695/)
12. Wojciechowska A, Braniewska A, Kozar-Kamińska K. MicroRNA in cardiovascular biology and disease. *Adv Clin Exp Med.* 2017; 26:865–74.  
<https://doi.org/10.17219/acem/62915> PMID:[29068585](https://pubmed.ncbi.nlm.nih.gov/29068585/)
13. Rupaimoole R, Slack FJ. MicroRNA therapeutics: towards a new era for the management of cancer and other diseases. *Nat Rev Drug Discov.* 2017; 16:203–22.  
<https://doi.org/10.1038/nrd.2016.246> PMID:[28209991](https://pubmed.ncbi.nlm.nih.gov/28209991/)
14. Vishnoi A, Rani S. MiRNA biogenesis and regulation of diseases: an overview. *Methods Mol Biol.* 2017; 1509:1–10.  
[https://doi.org/10.1007/978-1-4939-6524-3\\_1](https://doi.org/10.1007/978-1-4939-6524-3_1) PMID:[27826912](https://pubmed.ncbi.nlm.nih.gov/27826912/)
15. Xiong W, Ran J, Jiang R, Guo P, Shi X, Li H, Lv X, Li J, Chen D. miRNA-320a inhibits glioma cell invasion and migration by directly targeting aquaporin 4. *Oncol Rep.* 2018; 39:1939–47.  
<https://doi.org/10.3892/or.2018.6274> PMID:[29484417](https://pubmed.ncbi.nlm.nih.gov/29484417/)
16. Jiang Z, Yao L, Ma H, Xu P, Li Z, Guo M, Chen J, Bao H, Qiao S, Zhao Y, Shen J, Zhu M, Meyers C, et al. miRNA-214 inhibits cellular proliferation and migration in glioma cells targeting caspase 1 involved in pyroptosis. *Oncol Res.* 2017; 25:1009–19.  
<https://doi.org/10.3727/096504016X14813859905646> PMID:[28244850](https://pubmed.ncbi.nlm.nih.gov/28244850/)
17. Guled M, Lahti L, Lindholm PM, Salmenkivi K, Bagwan I, Nicholson AG, Knuutila S. CDKN2A, NF2, and JUN are dysregulated among other genes by miRNAs in Malignant mesothelioma -a miRNA microarray analysis. *Genes Chromosomes Cancer.* 2009; 48:615–23.  
<https://doi.org/10.1002/gcc.20669> PMID:[19396864](https://pubmed.ncbi.nlm.nih.gov/19396864/)
18. Hao J, Zhang S, Zhou Y, Hu X, Shao C. MicroRNA 483-3p suppresses the expression of DPC4/Smad4 in pancreatic cancer. *FEBS Lett.* 2011; 585:207–13.  
<https://doi.org/10.1016/j.febslet.2010.11.039> PMID:[21112326](https://pubmed.ncbi.nlm.nih.gov/21112326/)
19. Kuschnerus K, Straessler ET, Müller MF, Lüscher TF, Landmesser U, Kränkel N. Increased expression of miR-483-3p impairs the vascular response to injury in type 2 diabetes. *Diabetes.* 2019; 68:349–60.  
<https://doi.org/10.2337/db18-0084> PMID:[30257976](https://pubmed.ncbi.nlm.nih.gov/30257976/)
20. Menbari MN, Rahimi K, Ahmadi A, Mohammadi-Yeganeh S, Elyasi A, Darvishi N, Hosseini V, Abdi M. miR-483-3p suppresses the proliferation and progression of human triple negative breast cancer cells by targeting the HDAC8>oncogene. *J Cell Physiol.* 2020; 235:2631–42.  
<https://doi.org/10.1002/jcp.29167> PMID:[31508813](https://pubmed.ncbi.nlm.nih.gov/31508813/)
21. Jaraíz-Rodríguez M, Talaverón R, García-Vicente L, Pelaz SG, Domínguez-Prieto M, Álvarez-Vázquez A, Flores-Hernández R, Sin WC, Bechberger J, Medina JM, Naus CC, Tabernero A. Connexin43 peptide, TAT-Cx43266-283, selectively targets glioma cells, impairs Malignant growth, and enhances survival in mouse models in vivo. *Neuro Oncol.* 2020; 22:493–504.  
<https://doi.org/10.1093/neuonc/noz243> PMID:[31883012](https://pubmed.ncbi.nlm.nih.gov/31883012/)
22. Zhang X, Zhang X, Hu S, Zheng M, Zhang J, Zhao J, Zhang X, Yan B, Jia L, Zhao J, Wu K, Yang A, Zhang R. Identification of miRNA-7 by genome-wide analysis as a critical sensitizer for TRAIL-induced apoptosis in glioblastoma cells. *Nucleic Acids Res.* 2017; 45:5930–44.  
<https://doi.org/10.1093/nar/gkx317> PMID:[28459998](https://pubmed.ncbi.nlm.nih.gov/28459998/)
23. Wu K, Wang J, He J, Chen Q, Yang L. miR-483-3p promotes proliferation and migration of neuroblastoma cells by targeting PUMA. *Int J Clin Exp Pathol.* 2018; 11:490–501.  
PMID:[31938135](https://pubmed.ncbi.nlm.nih.gov/31938135/)
24. Wang C, Sun Y, Wu H, Yu S, Zhang L, Meng Y, Liu M, Yang H, Liu P, Mao X, Lu Z, Chen J. Elevated miR-483-3p expression is an early event and indicates poor prognosis in pancreatic ductal adenocarcinoma. *Tumour Biol.* 2015; 36:9447–56.  
<https://doi.org/10.1007/s13277-015-3690-x> PMID:[26124009](https://pubmed.ncbi.nlm.nih.gov/26124009/)
25. Khan AQ, Ahmed EI, Elareer NR, Junejo K, Steinhoff M, Uddin S. Role of miRNA-regulated cancer stem cells in the pathogenesis of human Malignancies. *Cells.* 2019; 8:840.  
<https://doi.org/10.3390/cells8080840> PMID:[31530793](https://pubmed.ncbi.nlm.nih.gov/31530793/)
26. Xue J, Zhou A, Wu Y, Morris SA, Lin K, Amin S, Verhaak R, Fuller G, Xie K, Heimberger AB, Huang S. miR-182-5p induced by STAT3 activation promotes glioma tumorigenesis. *Cancer Res.* 2016; 76:4293–304.  
<https://doi.org/10.1158/0008-5472.CAN-15-3073> PMID:[27246830](https://pubmed.ncbi.nlm.nih.gov/27246830/)
27. Johnson DE, O’Keefe RA, Grandis JR. Targeting the IL-6/JAK/STAT3 signalling axis in cancer. *Nat Rev Clin Oncol.* 2018; 15:234–48.  
<https://doi.org/10.1038/nrclinonc.2018.8> PMID:[29405201](https://pubmed.ncbi.nlm.nih.gov/29405201/)
28. Ligorio M, Sil S, Malagon-Lopez J, Nieman LT, Misale S, Di Pilato M, Ebright RY, Karabacak MN, Kulkarni AS, Liu A, Vincent Jordan N, Franses JW, Philipp J, et al. Stromal microenvironment shapes the intratumoral architecture of pancreatic cancer. *Cell.* 2019; 178:160–75.e27.  
<https://doi.org/10.1016/j.cell.2019.05.012> PMID:[31155233](https://pubmed.ncbi.nlm.nih.gov/31155233/)

## SUPPLEMENTARY MATERIAL

### Supplementary Table

Please browse Full Text version to see the data of Supplementary Table 1.

**Supplementary Table 1. Target Scan predicted the target genes of miR-483-3p.**